Thermochromism and Structural Change in Polydiacetylenes Including Carboxy and 4-Carboxyphenyl Groups as the Intermolecular Hydrogen Bond Linkages in the Side Chain

Chiaki Tanioku,[†] Kimihiro Matsukawa,[†,‡] and Akikazu Matsumoto*[,†]

[†]Department of Applied Chemistry and Bioengineering, Graduate School of Engineering, Osaka City University, 3-3-138 Sugimoto, Sumiyoshi-ku, Osaka 558-8585, Japan

[‡]Osaka Municipal Technical Research Institute, 1-6-50 Morinomiya, Joto-ku, Osaka 536-8533, Japan

Ⓢ Supporting Information

ABSTRACT: We investigated the thermochromic behavior of polydiacetylenes including the carboxy and 4-carboxyphenyl groups as the side-chain substituents adjacent to the conjugated main chain, and then, the thermal stability and the thermochromism reversibility of the polymers were related to changes in the polymer conformations monitored by IR and Raman spectroscopies and powder X-ray diffractions. The polydiacetylenes with no or a phenylene spacer between the main chain and the carboxylic acid moiety were revealed to exhibit a thermal resistance for maintaining reversible thermochromism in a high temperature range, rather than polydiacetylenes with a conventional structure with a flexible alkylene spacer. The molecular stacking structures of the diacetylenes and the corresponding polymers in the crystals were discussed based on the results of an X-ray single-crystal structure analysis as well as the powder X-ray diffraction measurements.

KEYWORDS: conjugated polymer, polydiacetylene, thermochromism, hydrogen bond, solid-state polymerization, topochemical polymerization, powder X-ray diffraction, IR spectroscopy, Raman spectroscopy, X-ray single crystal structure analysis
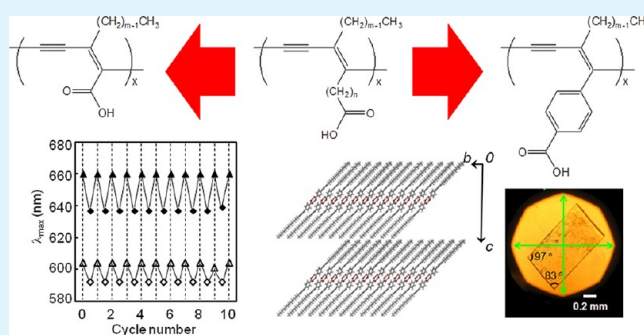
■ INTRODUCTION

Conjugated polymers have attracted significant attention because of their eminent electronic and chromatic properties applied to organic light-emitting diodes, photovoltaic cells, organic field-effect transistors (OFET), nonlinear optical materials, and chemical and biosensing.[1] Polydiacetylenes (PDAs), which are synthesized by the solid-state polymerization of diacetylene compounds during UV, X-ray, γ-ray, and electron beam irradiations, show drastic changes in their optical absorption and fluorescence properties under applied external stimuli such as temperature, pressure, light, ions, and biochemicals.[2−10] Recently, Adachi and coworkers reported that the UV and EB-radiation polymerization of 10,12-pentacosadiynoic acid (12,8-DA-CO$_2$H) deposited on a Si wafer having a thick SiO$_2$ layer produced the corresponding PDAs.[11,12] The obtained conjugated polymer crystals were applied as the organic semiconductor material for OFET devices.[11−17] The carrier mobility depended on the polymerization method, that is, UV or EB-radiation polymerization, and the conductive property of the PDAs was reduced by reduced quality of the polymer crystals due to the applied voltage and thermal deformation accompanying the transition from a blue phase to a red one.[12,13] Further modifications are demanded for the design of the repeating unit structure of the PDAs to guarantee excellent thermal stability and reversible thermo-

chromism for uses in various application fields including OFET. It has been reported that directly phenyl-substituted diacetylenes produced no polymers except for a few examples,[18−23] but we previously found that 1,3-alkadiynyl-4-benzoic acid (m,Ph-DA-CO$_2$Hs) and their naphthylmethylammonium derivatives could undergo a solid-state polymerization and provide the corresponding PDAs.[24,25] By the introduction of a conjugated substituent to the side chain, the obtained polymers showed absorption properties different from those of poly(alkadiynoic acid)s, that is, poly(m,n-DA-CO$_2$H)s with an alkylene spacer, and of poly(m,0-DA-CO$_2$H)s with no spacer between the main chain and the carboxylic acid. We considered that the poly(m,0-DA-CO$_2$H)s and poly(m,Ph-DA-CO$_2$H)s would have a thermal resistance for exhibiting a reversible thermochromism due to their rigid chain structures and the intermolecular hydrogen bonding by the formation of a carboxylic acid dimer (Figure 1). In this study, we investigated the thermochromism and structural changes in poly(m,0-DA-CO$_2$H)s and poly(m,Ph-DA-CO$_2$H)s to improve the thermal resistance and reversibility of the chromic properties, rather than poly(m,n-DA-CO$_2$H)s as the conventional PDAs. We
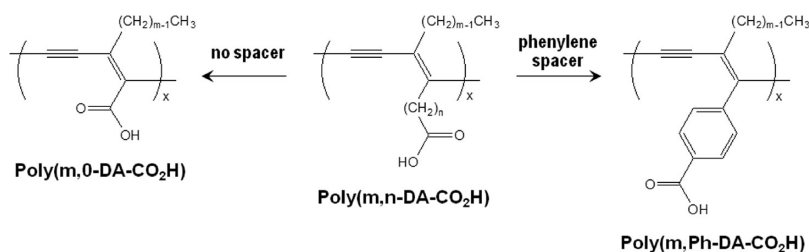
Figure 1. Molecular design to control reversible thermochromism for the PDAs including carboxylic acid as the intermolecular hydrogen bond linkage in the side chain.
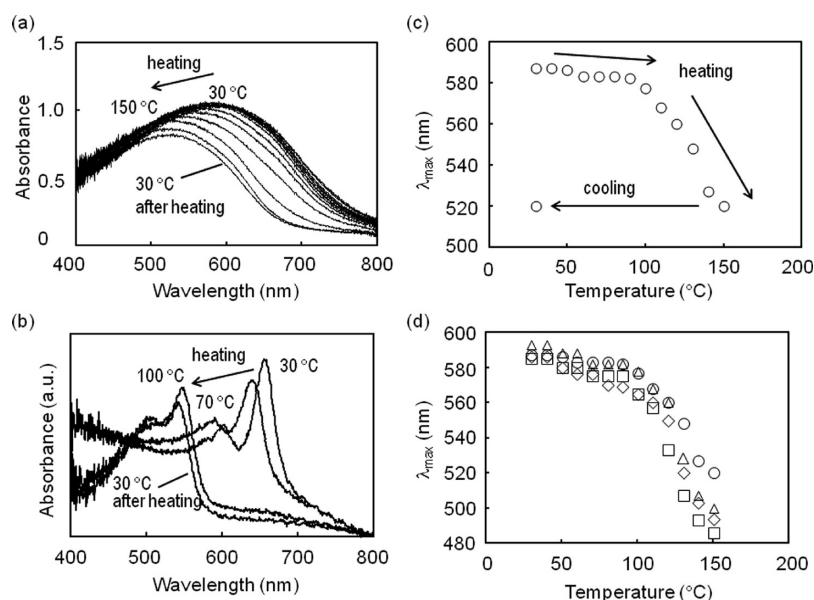

Figure 2. (a) Temperature dependence of the absorption spectrum of poly(10,0-DA-CO$_2$H) upon heating from 30 to 150 °C. (b) Temperature dependence of the absorption spectrum of poly(12,8-DA-CO$_2$H) upon heating from 30 to 100 °C. (c) Changes in the λ_{max} value of poly(10,0-DA-CO$_2$H) during the heating and cooling processes. (d) Change in the λ_{max} values of the poly(m,0-DA-CO$_2$H)s upon heating: $m = 10$ ($\Diamond$), 12 ($\triangle$), 14 ($\bigcirc$), and 16 ($\square$).

discuss the absorption properties of the PDAs with a carboxylic acid in the side chain, which are shown in Figure 1, under various temperature conditions, based on the results of the UV-vis absorption spectroscopy, powder X-ray diffraction, IR and Raman spectroscopies, differential scanning calorimetry (DSC), and an X-ray single-crystal structure analysis.

EXPERIMENTAL SECTION

General Procedures. The UV-vis spectra and optical microscope images were recorded using a Nikon Eclipse E600-POL spectrophotometer equipped with a Hamamatsu PMA-11 detector under temperature control using a Mettler Toledo FP900 and FP82HT. The FT-IR spectra were recorded using a Jasco FT/IR 430 spectrometer equipped with a Jasco Intron IRT-30 infrared microscope and a Mettler Toledo FP900 temperature controller. The Raman spectra were recorded using a Jasco NRS-3100 equipped with a Rinkam FTIR600 stage and a Japan Hightech K500-FVL temperature controller. The DSC measurements were carried out using Seiko DSC-6200 at the heating and cooling rates of 10 °C/min. The powder X-ray diffraction profile was recorded by a Rigaku RINT Ultima-2100 with monochromatized Cu Kα radiation (1.54184 Å; 40 kV; 40 mA; scan speed, 1−2°/min; scan step, 0.02°; scan angle, 2−40°) and equipped with a high-resolution parallel-beam optics system consisting of a PSA100U parallel slip analyzer and a 2960C1 graded multiplayer. The temperature was controlled using a PTC-20A controller. The scanning electron microscopy (SEM) observations were carried out using a Keyence VE6800 and VE9800 with an accelerating voltage source of

1.0−1.5 and 20 kV for the morphology observations and electron beam-radiated polymerization, respectively. The sample was coated with gold using an MSP-1S Vacuum Device magnetron sputter for 40 s at room temperature. Digital-scope microphotographs were taken using a Keyence VK-8700 laser microscope. The single-crystal X-ray diffraction data were collected using a Rigaku VariMax Saturn 724 diffractometer with multilayer mirror monochromated Mo Kα radiation (λ = 0.71075 Å, 50 kV, 24 mA) at −180 °C. The crystal structures were solved by a direct method using SHELX-97 and refined by the full-matrix least-squares method on F^2 with anisotropic displacement parameters for the nonhydrogen atoms using SHELXL-97. The DFT calculations were carried out using the Wave Function Spartan'08 software package. A semiempirical molecular orbital method was used for determination of the preferred conformations. The energies for the optimized structures were calculated at the B3LYP level of theory with the base functions of 6-31G*.

Polymerization. The m,0-DA-CO$_2$H and mPh-DA-CO$_2$H monomers were synthesized by the previously reported method.[24] Commercially available 12,8-DA-CO$_2$H was used after recrystallization. The γ-radiation was carried out at a radiation dose of 200 kGy using ^{60}Co at the Osaka Prefecture University. The polymer yield was determined from the weight of the polymers isolated as the insoluble part in chloroform or by IR spectroscopy. The conversion of the monomer to polymer was 30−73%.

RESULTS AND DISCUSSION

Poly(m,0-DA-CO$_2$H)s. The polymerization of the m,0-DA-CO$_2$Hs (m = 10, 12, 14, and 16), which were colorless and

powdery crystals, was carried out in the solid state under γ-radiation at a radiation dose of 200 kGy. The blue poly(m,0-DA-CO$_2$H) crystals were obtained after polymerization. They immediately turned to red when the unreacted monomer was removed by immersing the polymers in solvents such as chloroform and methanol. This is due to the collapse of polymer crystal structures by the elimination of monomer molecules from the product polymer crystals. Therefore, we investigated the thermochromism of the obtained poly(m,0-DA-CO$_2$H) crystals as the mixture of the resulting polymer and the remaining monomer without separating them after polymerization. It should be noted that Schott and coworkers[26−28] previously used the polymer crystal samples obtained at a low conversion to elucidate the electronic properties of conjugated polymers including various PDAs. We confirmed that the conversion of the monomer to polymer was as high as 73% during the polymerization of 10,0-DA-CO$_2$H in this study, based on the results of the gravimetric and IR spectroscopic determinations. We also checked no occurrence of the thermally-induced solid-state polymerization of 10,0-DA-CO$_2$H during the heating process for the investigation of the thermochromic properties of the resulting polymer. In the DSC curves of the polymerization products, the melting and crystallization of the monomer molecules were not observed (the melting point of 10,0-DA-CO$_2$H was 51 °C). Similar results were observed for the other m,0-DA-CO$_2$Hs. This indicates the formation of a solid solution consisting of monomer and polymer molecules during the solid-state polymerization, as expected from the homogeneous polymerization mechanism reported in the literature.[29,30]

Figure 2a shows the temperature dependence of the visible absorption spectra of poly(10,0-DA-CO$_2$H). The broad absorption band with a maximum absorption wavelength (λ_{max}) at 585 nm was observed at room temperature. Similar broad spectra were observed for the other poly(m,0-DA-CO$_2$H)s and the corresponding naphthylmethylammonium salts, which have no alkylene spacer between the conjugated main chain and a carboxylic acid moiety, while the poly(12,8-DA-CO$_2$H) that includes both an alkyl substituent and an alkylene spacer provided the typical absorption pattern consisting of a strong and sharp absorption band due to parallel polarization in the higher wavelength region as well as the smaller vibronic absorption bands in the higher energy region (Figure 2b). The broadening of the spectra is ascribed to intermolecular interactions between the conjugated polymer chains because the main chains of the poly(m,0-DA-CO$_2$H)s are closely connected to the adjacent main chain through the carboxylic acid dimer linkage without an alkylene spacer. The λ_{max} value of poly(10,0-DA-CO$_2$H) slightly decreased upon heating to 80 °C, and further heating led to a drastic change in the λ_{max} value, as shown in Figure 2a,c. The λ_{max} value reached 520 nm at 150 °C. The spectrum change was reversible in the temperature range of 30−80 °C but changed to an irreversible one when the polymer was heated over 100 °C. No change in the spectrum was observed when the polymer was cooled to 30 °C. A similar peak shift and color change were observed for all of the poly(m,0-DA-CO$_2$H)s, independent of the carbon chain length of the alkyl groups in the side chain (Figure 2d).

We investigated the structural changes in the PDAs using IR and Raman spectroscopies under temperature control. Figure 3 shows the changes in the IR and Raman spectra of poly(10,0-DA-CO$_2$H) during the heating and cooling processes. The absorption band due to the carbonyl stretching vibration of the
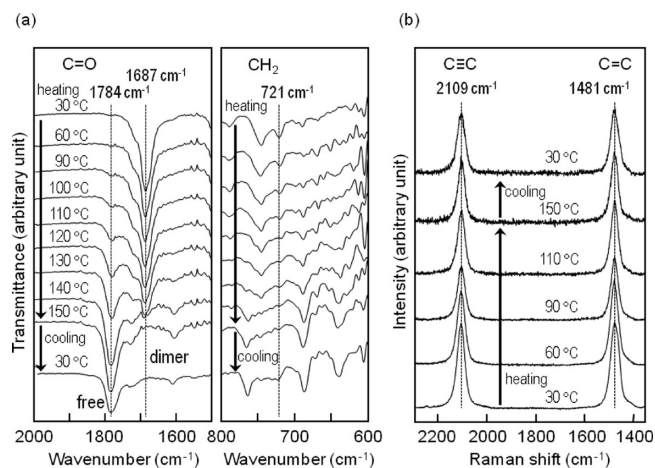

Figure 3. (a) Changes in the stretching vibration of the carbonyl group and the rocking vibration of the alkyl group in the FT-IR spectrum of poly(10,0-DA-CO$_2$H) during the heating and cooling processes. (b) Change in Raman spectrum due to the symmetric stretching vibrations of the carbon-to-carbon triple and double bonds of poly(10,0-DA-CO$_2$H) during the heating and cooling processes.

carboxylic acid, which intermolecularly forms a dimer by robust hydrogen bonding, was observed at 1687 cm^{-1} when the IR spectrum was recorded at room temperature. As the temperature increased, the peak intensity at 1687 cm^{-1} decreased, and an additional peak appeared at 1784 cm^{-1} due to a free carboxylic acid at temperatures over 90 °C. No shift was observed in the absorption band when the temperature was lowered from 150 to 30 °C, indicating the occurrence of an irreversible change in the hydrogen-bonding structure during heating. The intensity of the peak due to the rocking vibration of the trans-zigzag polymethylene group observed at 721 cm^{-1} gradually decreased upon heating from 30 °C, and it disappeared at 100 °C. This intensity change was partly reversible. On the other hand, no change was observed in the Raman spectrum of the same polymer (Figure 3b). The Raman bands observed at 2109 and 1481 cm^{-1} due to the C≡C and C=C bonds, respectively, showed no shifts in the temperature range of 30−150 °C during both the heating and the cooling processes. These vibration spectroscopic experiments suggest a drastic and irreversible change in the side-chain conformation and the maintenance of the rigid main-chain conjugated structure at high temperatures.

The chromatic changes in the PDAs as well as other conjugated polymers due to external stimuli have been discussed in relation to the electronic properties of the polymers.[31−38] The change in the visible spectrum from the blue phase to the red one indicates a conformational change in the conjugated structure of the PDAs, but simultaneously, the nonchanging Raman spectrum in this study suggests an immutable bond structure and strength for the multiple bonds in the main chain. Recently, Filhol and Schott et al.[28] reported that torsional isomers with a twist in the lateral groups existed in the PDA crystals, and the experimental results reported in the literature, such as the absorption, Raman, and NMR spectra, were well explained by their models and DFT calculation results. This isomerism modifies the electronic structure of the PDAs and induces a shift in the absorption peaks but insensitive to the vibration bands such as Raman shifts. It can be concluded that the poly(m,0-DA-CO$_2$H)s also have isomeric conformations with small energetic differences

942

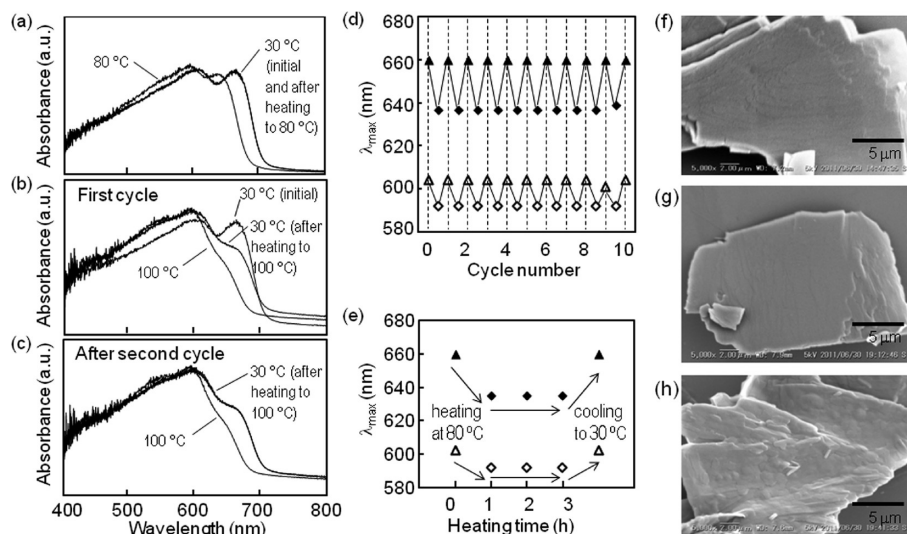dx.doi.org/10.1021/am302603p | ACS Appl. Mater. Interfaces 2013, 5, 940−948

Figure 4. Change in the visible absorption spectra of poly(16,Ph-DA-CO$_2$H) (a) during the heating and cooling processes in the temperature range between 30 and 80 °C, (b) during the heating and cooling processes in the temperature range between 30 and 100 °C for the first cycle, and (c) during the heating and cooling processes in the temperature range between 30 and 100 °C after the second cycle. (d) Reversible change in the λ_{max} values of poly(16,Ph-DA-CO$_2$H) at 30 (triangles) and 80 °C (squares). The spectra were recorded with an interval of 10 min for the temperature change to equilibrate. (e) Change in the λ_{max} values of poly(16,Ph-DA-CO$_2$H) after a 3 h heating at 80 °C. Triangles and squares denote the data obtained at 30 and 80 °C, respectively. SEM images of poly(16,Ph-DA-CO$_2$H) (f) before heating, (g) after heating to 80 °C, and (h) after heating to 100 °C. The images of panels g and h were recorded at 30 °C.
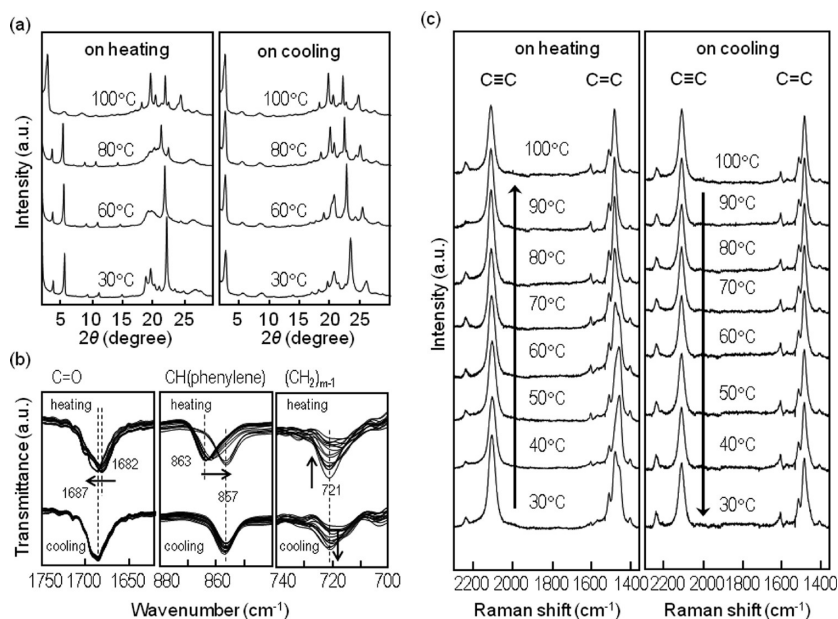

Figure 5. (a) Powder X-ray diffraction profiles of poly(16,Ph-DA-CO$_2$H) during the heating and cooling processes between 30 and 100 °C. (b) Change in the stretching vibration of the carbonyl group, the deformation vibration of CH in the phenylene group, and the rocking vibration of the methylene group in the FT-IR spectrum of poly(16,Ph-DA-CO$_2$H) during the heating and cooling processes in the temperature range between 30 and 100 °C. (c) Change in the Raman spectrum of poly(16,Ph-DA-CO$_2$H) during the heating and cooling processes in the temperature range between 30 and 100 °C.

and show irreversible changes in the structure and chromatic properties.

Poly(m,Ph-DA-CO$_2$H)s. The effect of a phenylene spacer between the conjugated main chain and the carboxylic acid in the side chain on the chromatic change in the PDAs was investigated. Figure 4a shows a change in the visible absorption spectra of poly(16,Ph-DA-CO$_2$H) during the heating and cooling processes in the temperature range between 30 and 80 °C. In this range, the absorption spectrum was completely

reversible, and the same spectrum was obtained after heating to 80 °C. The plots in Figure 4d,e show a reversible spectral change during many repeated cycles and also for a long heating time. These results indicated the excellent thermal stability and reversibility of the thermochromism due to a robust poly-(16,Ph-DA-CO$_2$H) structure. The structural change mode sensitively depended on the upper temperature limit. Upon further heating to 100 °C, the polymer became like the other conformation, which was different from the polymer structure
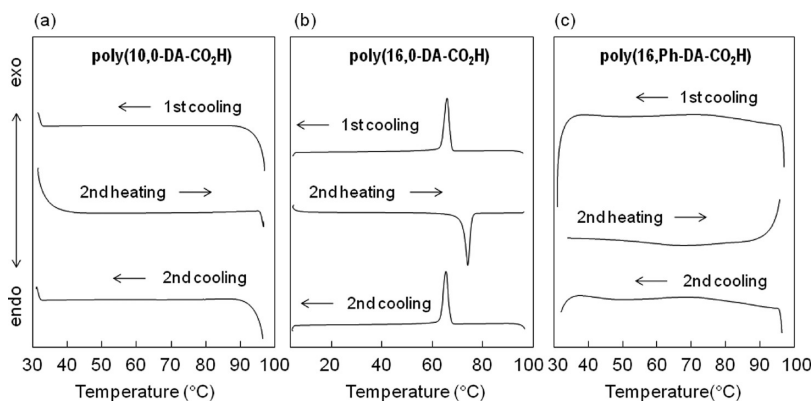
Figure 6. DSC traces for poly(m,0-DA-CO$_2$H)s and poly(16,Ph-DA-CO$_2$H) prepared by γ-radiation polymerization. (a) poly(10,0-DA-CO$_2$H), (b) poly(16,0-DA-CO$_2$H), and (c) poly(16,Ph-DA-CO$_2$H) scanned in the temperature range of 30−100 °C at the heating and cooling rates of 10 °C/min.

observed at 30 °C as the initial stage, accompanying an irreversible change in the absorption spectrum (Figure 4b). The spectrum reversibly changed in the 30−100 °C range after the second cycle, as shown in Figure 4c. The morphology of the poly(16,Ph-DA-CO$_2$H) crystals was compared before and after heating (Figure 4f−h). No morphology change was observed in the SEM images of the crystal surfaces after the temperature was raised to 80 °C, while the coarseness of the surface structure increased at 100 °C. This suggests a drastic change in the crystal structure upon heating over 80 °C.

The occurrence of a phase transition was confirmed by a discontinuous change in the powder X-ray diffraction profile (Figure 5a). The transition observed in the temperature range between 80 and 100 °C was irreversible, and the diffraction profiles showed no change in the cooling process. In the IR spectrum (Figure 5b), the C═O stretching vibration observed at 1682 cm^{-1} irreversibly shifted to 1687 cm^{-1}. Similarly, the wavenumber of the CH deformation vibration also changed from 863 to 857 cm^{-1} in an irreversible fashion.

For the CH$_2$ rocking vibration, no wavenumber shift occurred with the partial reversibility of the intensity change. On the basis of the thermal histories of the IR absorption bands, it has been revealed that the conformation of the phenylene spacer and the carboxylic acid dimer structure irreversibly changed, while the trans-zigzag structure of the methylene units in the alkyl side chain was partly reversible due to the alkyl-chain packing during the side-chain melting and partial crystallization. The temperature dependence of the Raman spectrum also produced a similar conclusion. The Raman bands due to the C═C bond of poly(16,Ph-DA-CO$_2$H) in Figure 5c consisted of several absorption bands because the polymer has complicated isomeric structures due to the presence of a conjugated phenylene substituent in the side chain. The band due to the vibration of a carbon-to-carbon double bond in the main chain irreversibly changed during the heating process. The intensity of the peak at the lowest Raman shift (1557 cm^{-1}) decreased upon heating but underwent no change during the subsequent cooling process. The changes in the IR and Raman spectra and X-ray diffraction were irreversible during heating up to 100 °C, while they were reversible in the temperature range below 80 °C. In our previous study,[24] we revealed that the poly(m,Ph-DA-Naph)s, which are the naphthylmethylammonium salts of the poly-(m,Ph-DA-CO$_2$H)s, showed a thermochromic behavior different from that of the poly(m,0-DA-Naph)s, which is the

naphthylmethylammonium salts of the poly(m,0-DA-CO$_2$H)s. The absorption intensity at the higher wavelength gradually decreased, and the intensity of the shorter band simultaneously increased with an isosbestic point. No shift in the peak top was observed below 90 °C, and the switching of the conjugation between the aromatic substituent and the conjugated polymer backbone occurred during the temperature change from 0 to 100 °C. These results also support the conclusion that the conjugating system of the poly(m,Ph-DA-CO$_2$H)s irreversibly changes at a temperature over 90 °C upon heating. Figure 6 shows the DSC traces for the poly(m,0-DA-CO$_2$H)s and poly(16,Ph-DA-CO$_2$H) observed in the temperature range from room temperature to 100 °C. No peak was detected in the DSC trace of poly(10,0-DA-CO$_2$H) during the heating and cooling processes. When the alkyl chain length of the side chain increased, the peaks due to the melting and crystallization of the long alkyl groups appeared around 70 °C. Similar reversible transitions were also observed for poly(16,Ph-DA-CO$_2$H) in the scanning range below 80 °C, but they diminished when the temperature was once raised to 100 °C. These results suggest that the structural changes observed by the IR, Raman, and absorption spectroscopies are due to a dynamic change in the main-chain conformation in the polymer crystal lattice, but they cannot be explained by a simple crystal-to-crystal or crystal-to-amorphous transition mechanism.

Crystal Structure Determination. The single crystals of the 12,Ph-DA-CO$_2$H monomer were prepared by the slow evaporation of the mixed solvent of n-hexane and diethyl ether from the solutions at room temperature. Colorless and thin plate crystals were obtained (thickness, ca. 10 μm) and used for the X-ray single-crystal structure determination. The X-ray diffraction data were collected at −180 °C to avoid the occurrence of polymerization during the X-ray radiation. The obtained crystal parameters are summarized in Table 1. The optical microscope image of the 12,Ph-DA-CO$_2$H crystal and the packing structures of the molecules in the crystal are shown in Figure 7a,b. The 12,Ph-DA-CO$_2$H molecules exist as the carboxylic acid dimers, and they form a layer structure on the ab plane of the crystal. The diacetylene moieties are aligned along the a-axis with a tilt angle of ca. 45°. The direction of the diacetylenes bond agreed with one of the optic axes shown in Figure 7a (vertical one). The methylene unit adjacent to the diacetylene of 12,Ph-DA-CO$_2$H had a gauche conformation, while the others were trans. This conformation results in the bend angle of 148.1° between a diacetylene moiety and an alkyl

Table 1. Crystal Parameters for 12,Ph-DA-CO₂H

formula	$C_{23}H_{30}O_2$	Z	2
formula weight	338.49	ρ (g cm⁻³)	1.168
crystal dimensions (mm)	0.350 × 0.250 × 0.010	μ (Mo Kα) (cm⁻¹)	0.723
crystal habit	platelet	unique reflns	24225
crystal system	triclinic	observed reflns	3247
space group	$P\bar{1}$(#2)	no variables	228
a (Å)	4.582(4)	R_1 [$I > 2.00\sigma(I)$]	0.0596
b (Å)	5.431(5)	wR_2	0.171
c (Å)	39.03(4)	max peak in final diff map (e⁻ Å⁻³)	0.24
α (degree)	88.59(2)	min peak in final diff map (e⁻ Å⁻³)	−0.31
β (degree)	87.51(2)	goodness of fit indicator	1.065
γ (degree)	82.76(2)	max shift/error	0.000
V (Å³)	962(2)	temperature (°C)	−180

chain of the 12,Ph-DA-CO₂H molecule (Figure 7d) in the crystals, being similar to the conformation determined for an isolated single molecule by the DFT calculations (146.4°). A small difference in these bend angle values is due to the intermolecular interaction for the alkyl-chain packing in the crystals. Similar layer-stacking structures were confirmed for the series of m,Ph-DA-CO₂H and m,0-DA-CO₂H crystals based on the powder X-ray diffraction profiles in Figure 8. Several diffractions expected for the series of planes of layered crystals were observed for all of the compounds. The slopes of the lines of the alkyl-chain length dependence of the interlayer distance in Figure 9 indicate a similar molecular stacking structure for the m,Ph-DA-CO₂H and m,0-DA-CO₂H series. The identical slopes of the lines for both series in Figure 9 indicate a stacking structure with identical tilt angles of the alkyl chains against the layers in the crystals. From the change in the d-value along with an increase in the m number, the tilt angle is estimated to be 44°,[24,39] well agreeing with the results for the single-crystal structure analysis of 12,Ph-DA-CO₂H. The polymer crystals
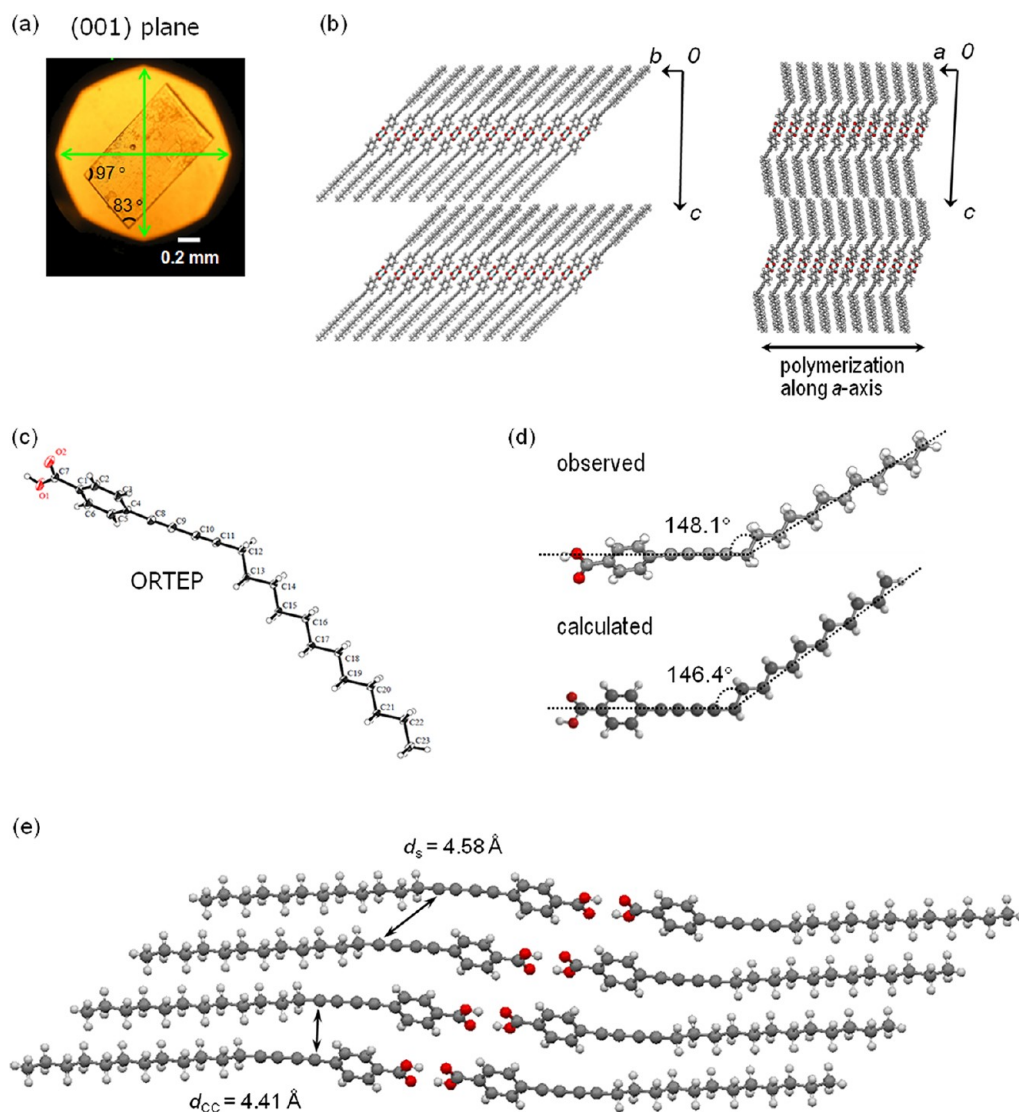

Figure 7. Crystal structure of 12,Ph-DA-CO₂H. (a) Optical macroscope image of the (001) plane of the crystal. Arrows indicate optic axes. (b) Molecular packing structures in the crystal viewed along the a- and b-axes, (c) ORTEP, and (d) molecular conformations determined by X-ray single-crystal structure analysis and DFT calculations. (e) Monomer stacking structure determined by X-ray single-crystal structure analysis. d_s, stacking distance; d_{CC}, carbon-to-carbon distance.
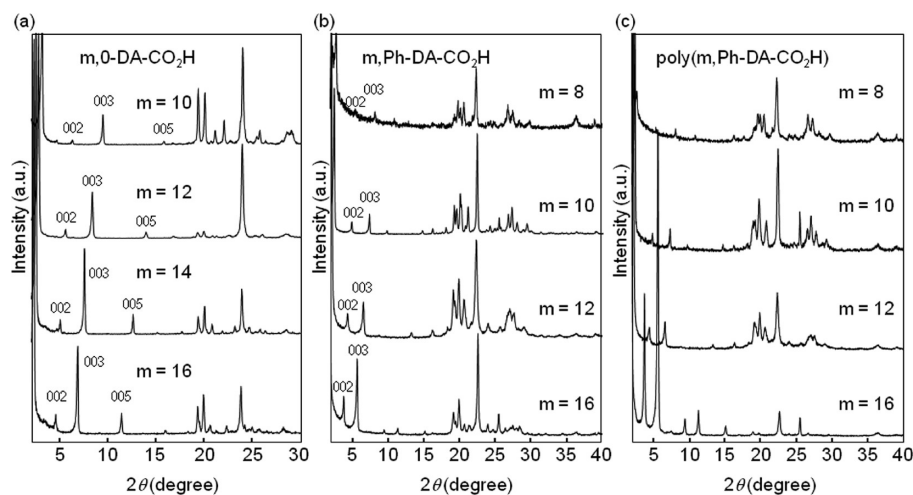
Figure 8. Powder X-ray diffraction profiles for (a) m,0-DA-CO$_2$H monomer crystals measure at -120 °C, (b) m,Ph-DA-CO$_2$H monomer crystals measured at room temperature, and (c) poly(m,Ph-DA-CO$_2$H) crystals measured at room temperature.
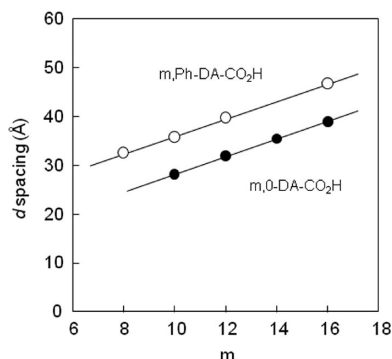

Figure 9. Plots of d spacing values for m,0-DA-CO$_2$H (●) and m,Ph-DA-CO$_2$H (○) monomer crystals.

provided diffraction profiles (Figure 8c) similar to the corresponding monomer crystals, indicating that the polymerization surely proceeded via a topochemical polymerization mechanism.

The lattice length of the a-axis (4.582 Å) determined by X-ray single crystal analysis at -180 °C, that is, the stacking distance of the 12,Ph-DA-CO$_2$H molecules for topochemical polymerization, was slightly smaller than the ideal value (4.8 Å).[29] On the basis of the results of the powder X-ray diffraction measurements at room temperature, small changes in the crystal lattice structures were observed during the polymerization; for example, the stacking distance value (d_s) of the 12,Ph-DA-CO$_2$H molecules ($2\theta = 19.22°$, $d = 4.61$ Å) along the a-axis in the monomer crystals was similar to the fiber period of the poly(12,Ph-DA-CO$_2$H) crystals ($2\theta = 19.14°$, $d = 4.63$ Å), and the layer distance ($d = 39.8$ Å) did not change during the polymerization as shown in Figures 8 and S3 in the Supporting Information. A carbon-to-carbon distance (d_{CC}) to make a new covalent bond during the polymerization was estimated to be 4.41 Å, as shown in the stacking structure of 12,Ph-DA-CO$_2$H molecules (Figure 7e). This value was similar to those reported for the other diacetylene compounds, which can undergo solid-state polymerization.[2,6,29,40−43] In fact, the solid-state polymerization of m,Ph-DA-CO$_2$Hs slowly occurs, while the m,0-DA-CO$_2$Hs and m,n-DA-CO$_2$Hs immediately turn blue when they were stood under scattered light at room temperature. We previously reported that the stacking distance of the monomer

molecules in the crystals determines the rate of polymerization during the solid-state polymerization of the diene monomers.[44,45] The smaller the difference in the actual stacking distance and the ideal one, that is, the fiber period of the resulting polymer, the faster the polymerization rate during the polymerizations accompanying the shrinking and expanding of the crystal lattice along the polymerization axis. The slow polymerization process of m,Ph-DA-CO$_2$Hs is due to the rigid structure of the monomer molecules including the phenyl ring adjacent to the diacetylenes bond.

In this study, the polymerization by γ-ray and electron beam radiations led to an expansion of the crystal along the a-axis direction. The deforming of the surface morphology with crack formation in a specific direction was observed, as shown in Figure 10. Many small cracks were detected on the crystal surface of 16,Ph-DA-CO$_2$H after the γ-radiation polymerization (Figure 10a,b). A clearer cracking pattern was produced in a direction orthogonal to the polymerization axis, independent of the scanning direction of the electron-beam radiation of 20 kV radiation voltage, which was enough to induce the solid-state polymerization of 16,Ph-DA-CO$_2$H (Figure 10c,d). The formation of cracks in the crystals is due to the shrinkage of the crystals during the polymerization. Kato et al.[12] recently reported the high carrier mobility in the PDA films polymerized by electron-beam radiation and referred to the morphology change of the crystal surface during the polymerization of 12,8-DA-CO$_2$H. The deformations of the thin crystals with the formation of bumps occurred in the first irradiation scanning, and the bumps were then squashed during the subsequent scanning, finally resulting in the formation of smooth surface without crack formation.[46] Shivashankar et al.[46] also pointed out that surface eruptions were observed during the γ-radiation polymerization of a diacetylenes monomer in the solid state in the presence of air, and they were produced due to the anisotropic polymerization at the specific crystal face. In this study, the formation of cracks on the surface was irreversibly produced in the absence of air by the deformation of the 12,Ph-DA-CO$_2$H crystals, and this is due to the rigid structure of the polymer crystals containing the phenylene moiety in the side chain. The m,0-DA-CO$_2$H monomers gave thinner platelet crystals (Figure 10e), and the 10,0-DA-CO$_2$H with the smallest alkyl substituent only resulted in fine crystals (Figure 10f), indicating that long-alkyl and rigid phenylene groups are
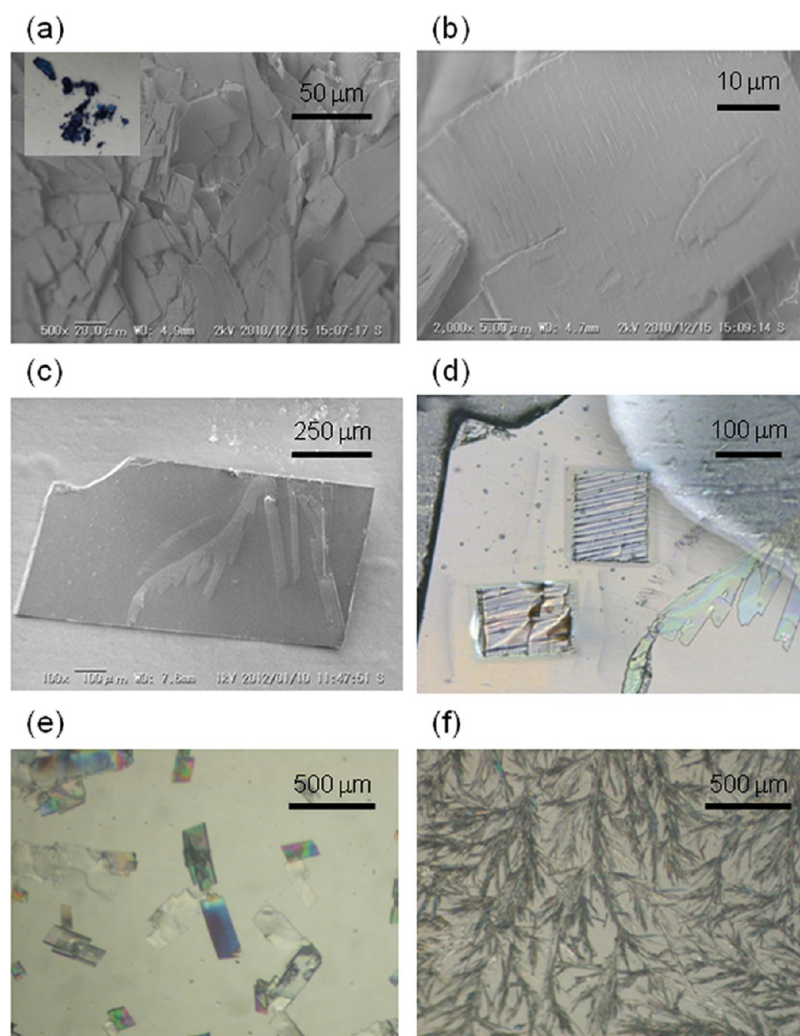
Figure 10. Microscopic images of the 16,Ph-DA-CO$_2$H and 12,Ph-DA-CO$_2$H crystals. (a, b) SEM images of 16,Ph-DA-CO$_2$H after γ-radiation polymerization. Inserted: photograph of 16,Ph-DA-CO$_2$H after γ-radiation polymerization. (c) SEM image of 12,Ph-DA-CO$_2$H before polymerization and (d) digital microscope image after polymerization by electron-beam radiation, which was carried out only in the rectangular areas (80 μm × 120 μm). Polarized optical microscope images of (e) 14,0-DA-CO$_2$H and (f) 10,0-DA-CO$_2$H.

needed for the large size platelet crystal growth. Crystal growth ability providing large-size platelet crystals as well as the thermal and electronic stabilities of the PDA single crystals will be required for the OFET applications in the future.

CONCLUSION

We investigated the thermochromism of poly(m,0-DA-CO$_2$H)s and poly(m,Ph-DA-CO$_2$H)s, which are the main-chain conjugated polymers with no or phenylene spacer between the main chain and a carboxylic acid in the side chain. These PDAs were thermally stable and exhibited a reversible thermochromism in a high temperature range, being different from the easy occurrence of an irreversible transition from a blue phase to the red one during the heating of the poly(m,n-DA-CO$_2$H)s including a flexible alkylene spacer. The rigid chain structure of poly(m,Ph-DA-CO$_2$H)s plays the role of maintaining the blue phase at a high temperature. The single-crystal structure of the 12,Ph-DA-CO$_2$H monomer was determined by an X-ray single crystal structure analysis at −180 °C. The molecular conformation and the layered packing structure of 12-Ph-DA-CO$_2$H in the crystals were revealed, and the other m-Ph,DA-CO$_2$Hs and m,0-DA-CO$_2$Hs as well as the

corresponding polymer crystals were confirmed to have a similar layer structure in the crystals, based on their powder X-ray diffraction profiles. Recently, it was reported that the m,Ph-DA-CO$_2$H monomers exhibited unique liquid crystalline mesomorphic properties including several discotic mesophases that were constructed by a hierarchical self-assembly of the rodlike diacetylene carboxylic acid dimers.[47] To control the molecular arrangement of diacetylene compounds using the mesomorphic properties and the polymerization behaviors in an anisotropic state, such as the liquid crystalline state and the solid state, will help in developing new organic semiconductors for electronics. We are continuing further investigations to control the alignment of the diacetylene monomers on substrates and their polymerization reactivity as well as the physical and electronic properties of the polymers.

ASSOCIATED CONTENT

S Supporting Information

CIF and powder X-ray diffraction data. This material is available free of charge via the Internet at http://pubs.acs.org.

■ AUTHOR INFORMATION

Corresponding Author

*Fax: +81-6-6605-2981. E-mail: matsumoto@a-chem.eng. osaka-cu.ac.jp.

Notes

The authors declare no competing financial interest.

■ REFERENCES

(1) Skothem, T. A., Reynolds, J. R., Eds. *Handbook of Conjugating Polymers*, 3rd ed.; CRC Press: New York, 2007.

(2) Zuilhof, H.; Barentsen, H. M.; van Dijk, M.; Sudhölter, E. J. R.; Hoofman, R. J. O. M.; Siebbeles, L. D. A.; de Haas, M. P.; Warman, J. M. *Supramolecular Photosensitive and Electroactive Materials*; Nalwa, H. S., Ed.; Academic Press: New York, 2001; pp 339−437 and references therein.

(3) Okada, S.; Peng, S.; Spevak, W.; Charych, D. *Acc. Chem. Res.* **1998**, *31*, 229−239.

(4) Reppy, M. A.; Pindzola, B. A. *Chem. Commun.* **2007**, *42*, 4317−4338.

(5) Ahn, D. J.; Kim, J.-M. *Acc. Chem. Res.* **2008**, *41*, 805−816.

(6) Lauher, J. W.; Fowler, F. W.; Goroff, N. S. *Acc. Chem. Res.* **2008**, *41*, 1215−1229.

(7) Yoon, B.; Lee, S.; Kim, J.-M. *Chem. Soc. Rev.* **2009**, *38*, 1958−1968.

(8) Sun, X.-M.; Chen, T.; Huang, S.-Q.; Li, L.; Peng, H. S. *Chem. Soc. Rev.* **2010**, *39*, 4244−4257.

(9) Chen, X.-Q.; Zhou, G. D.; Peng, X.-J.; Yoon, J. *Chem. Soc. Rev.* **2012**, *41*, 4610−4630.

(10) Yarimaga, O.; Jaworski, J.; Yoon, B.; Kim, J.-M. *Chem. Commun.* **2012**, *48*, 2469−2485.

(11) Nishide, J.; Oyamada, T.; Akiyama, S.; Sasabe, H.; Adachi, C. *Adv. Mater.* **2006**, *18*, 3120−3124.

(12) Kato, T.; Yasumatsu, M.; Origuchi, C.; Tsutsui, K.; Ueda, Y.; Adachi, C. *Appl. Phys. Express* **2011**, *4*, 091601.

(13) Zou, G.; Lim, E.; Tamura, R.; Kajimoto, N.; Manaka, T.; Iwamoto, M. *Jpn. J. Appl. Phys.* **2006**, *45*, 6436−6441.

(14) Lee, J. Y.; Aleshin, A. N.; Kim, D. W.; Lee, H. J.; Kim, Y. S; Wegner, G.; Enkelmann, V.; Roth, S.; Park, Y. W. *Synth. Met.* **2005**, *152*, 169−172.

(15) Takami, K.; Kuwahara, Y.; Ishii, T.; Kasaya, M. A.; Saito, A.; Aono, M. *Surf. Sci.* **2005**, *591*, L273−L279.

(16) Wilson, E. G. *Chem. Phys. Lett.* **1982**, *90*, 221−224.

(17) Donovan, K. J.; Wilson, E. G. *Philos. Mag.* **1981**, *B44*, 9−29.

(18) Baughman, R. H. *J. Appl. Phys.* **1972**, *43*, 4362−4370.

(19) Kojima, Y.; Matsuoka, T.; Takahashi, H. *J. Mater. Sci. Lett.* **1996**, *15*, 539−541.

(20) Sarkar, A.; Okada, S.; Nakanishi, H.; Matsuda, H. *Macromolecules* **1998**, *31*, 9174−9180.

(21) Sarkar, A.; Okada, S.; Matsuzawa, H.; Matsuda, H.; Nakanishi, H. *J. Mater. Chem.* **2000**, *10*, 819−828.

(22) Okuno, T.; Izuoka, A.; Ito, T.; Kubo, S.; Sugawara, T.; Sato, N.; Sugawara, Y. *J. Chem. Soc., Perkin Trans. 2* **1998**, 889−895.

(23) Chan, Y.-H.; Lin, J.-T.; Chen, I.-W. P.; Chen, C.-H. *J. Phys. Chem. B* **2005**, *109*, 19161−19168.

(24) Dei, S.; Shimogaki, T.; Matsumoto, A. *Macromolecules* **2008**, *41*, 6055−6065.

(25) Dei, S.; Matsumoto, A. *Macromol. Chem. Phys.* **2009**, *210*, 11−20.

(26) Schott, M. *Photophysics of Molecular Materials: From Single Molecules to Single Crystals*; Lanzani, G., Ed.; Wiley-VCH: Weinheim, 2006; pp 49−151.

(27) Schott, M. *J. Phys. Chem. B* **2006**, *110*, 15864−15868.

(28) Fihol, J.-S.; Deschamps, J.; Dutremez, S. G.; Boury, B.; Barisien, T.; Legrand, L.; Schott, M. *J. Am. Chem. Soc.* **2009**, *131*, 6976−6988.

(29) Enkelmann, V. *Adv. Polym. Sci.* **1984**, *63*, 91−136.

(30) Furukawa, D.; Matsumoto, A. *Macromolecules* **2007**, *40*, 6048−6056.

(31) Lam, J. W. Y.; Tang, B. Z. *Acc. Chem. Res.* **2005**, *38*, 745−754.

(32) Yoshino, K.; Morita, S.; Yin, X. H.; Kawai, T. *Jpn. J. Appl. Phys.* **1993**, *32*, L547−L549.

(33) Tachibana, H.; Hosaka, N.; Tokura, Y. *Macromolecules* **2001**, *34*, 1823−1827.

(34) Gelinck, G. H.; Warman, J. M.; Staring, E. G. J. *J. Phys. Chem.* **1996**, *100*, 5485−5491.

(35) Chen, S. A.; Chang, E. C. *Macromolecules* **1998**, *31*, 4899−4907.

(36) Nakanishi, N.; Tada, K.; Onoda, M. *Jpn. J. Appl. Phys. Part 1* **2000**, *39*, 1913−1917.

(37) Li, X. G.; Zhou, H. J.; Huang, M. R. *Polymer* **2005**, *46*, 1523−1533.

(38) Miller, R. D.; Michl, J. *Chem. Rev.* **1989**, *89*, 1359−1410.

(39) Shimogaki, T.; Matsumoto, A. *Macromolecules* **2011**, *44*, 3323−3327.

(40) Wang, X.; Sandman, D. J.; Enkelmann, V.; Chen, C.-H.; Foxman, B. M. *J. Macromol. Sci., Part A: Pure Appl. Chem.* **2008**, *45*, 914−916.

(41) Li, Z.; Fowler, F. W.; Lauher, J. W. *J. Am. Chem. Soc.* **2009**, *131*, 634−643.

(42) Deschamps, J.; Balog, M.; Boury, B.; Ben Yahia, M.; Hihol, J. S.; van der Lee, A.; Legrand, l.; Schott, M.; Dutremez, S. G. *Chem. Mater.* **2010**, *22*, 3961−3982.

(43) Hsu, T. J.; Fowler, F. W.; Lauher, J. W. *J. Am. Chem. Soc.* **2012**, *134*, 142−145.

(44) Matsumoto, A.; Tanaka, T.; Tsubouchi, T.; Tashiro, K.; Saragai, S.; Nakamoto, S. *J. Am. Chem. Soc.* **2002**, *124*, 8891−8902.

(45) Matsumoto, A.; Furukawa, D.; Mori, Y.; Tanaka, T.; Oka, K. *Cryst. Growth Des.* **2007**, *7*, 1078−1085.

(46) Shivashankar, V.; Sung, C.; Kumar, J.; Tripathy, S. K.; Sandman, D. J. *Acta Polym.* **1997**, *48*, 88−91.

(47) Shimogaki, T.; Dei, S.; Ohta, K.; Matsumoto, A. *J. Mater. Chem.* **2011**, *21*, 10730−10737.

948

dx.doi.org/10.1021/am302603p | *ACS Appl. Mater. Interfaces* 2013, 5, 940−948